EXPERIMENTAL RESULTS
WITH ATOMIC HYDROGEN STORAGE BEAM SYSTEMS*

Helmut Hellwig and Howard E. Bell

Atomic Frequency and Time Standards Section
National Bureau of Standards
Boulder, Colorado 80302 USA

Summary

Two atomic hydrogen storage beam devices are described, one based on the detection of hydrogen atoms, the other on the detection of changes in the microwave signal due to the hydrogen resonance.

Electron bombardment ionization is used for the detection of atomic hydrogen. Detector efficiencies of up to 5×10^{-4} are measured using a method which is based on the study of pulse decay at maser oscillation threshold. Quantitative measurements of the atomic hydrogen beam intensity as a function of source pressure and RF discharge power are given. The overall efficiency of the atomic hydrogen detection in the hydrogen storage beam device is estimated at about 10^{-8}. Ways to increase the efficiency are indicated.

The second device, which is based on microwave detection, closely resembles a hydrogen maser oscillator with a low-Q cavity below oscillation threshold. Cavity pulling can be reduced to a point where environmental temperature fluctuations limit the stability mainly via the second-order Doppler effect. A quartz crystal oscillator is locked to the hydrogen hyperfine transition using the dispersion of this resonance. Locking to the dispersion feature eliminates the need for frequency modulation in order to find line-center. The stability of the frequency standard was measured against crystal oscillators and cesium beam frequency standards; stabilities of 4×10^{-13} were recorded for sampling times of 30 seconds and of 3 hours.

Key Words (for information retrieval): Atomic hydrogen beam, Atomic hydrogen generation, Dispersion, Frequency stability, Frequency standard, Hydrogen atom detection, Hydrogen flux calibration, Hydrogen maser, Relaxation measurements, Spin exchange.

Introduction

As compared to the hydrogen maser oscillator, a passive hydrogen standard offers a significant reduction in cavity pulling [1], [2]. This, together with the elimination of the requirement to obtain self-oscillation, offers considerable design advantages, might lead to improved long-term stability, and possibly offers greater flexibility to evaluate the frequency bias due to wall-collisions of the stored hydrogen atoms (wallshift)[3].

Based on certain theoretical considerations, a hydrogen storage beam tube employing the detection of hydrogen atoms[1] is an appealing design [2], [5]. For such a device, operating far below oscillation threshold, the cavity pulling factor F_1 is very favorable [1], [6]:

$$F_1 = \left(\frac{Q_c}{Q_\ell} \right)^2 , \qquad (1)$$

where Q_c and Q_ℓ are the cavity and line quality factors, respectively. However, an efficient, low-background hydrogen detector is essential to exploit the advantage given by hydrogen atom detection as compared to the detection of the microwave power.

For a passive device, based on detecting the microwave signal which is transmitted through the cavity containing the hydrogen atoms, J. Viennet, C. Audoin, and M. Desaintfuscien have shown [1] that the cavity pulling factor F_2 is

$$F_2 = \frac{Q_c}{Q_\ell} \frac{1}{2 - \alpha} . \qquad (2)$$

Here, α is a gain parameter [for negligible saturation the gain is equal to $(1 - \alpha)^{-1}$ at resonance]. Information on the hydrogen line can be obtained by detecting either the microwave intensity or the dispersion signal. Since the dispersion signal contains the frequency information, its use avoids the need for frequency modulation of the slaved quartz crystal oscillator; however, the hydrogen flux has to be modulated in order to subtract--in first approximation--the dispersive characteristic of the microwave cavity.

In the following, we report in Part 1 our results with a system employing the detection of hydrogen atoms, and in Part 2 we discuss the design and performance of a system employing microwave signal detection.

1. Hydrogen Atom Detection

1.1 Beam intensity calibration

In order to evaluate the efficiency of an atomic hydrogen detector it is necessary to know the hydrogen beam intensity. We used a hydrogen maser oscillator to

*Contribution of the National Bureau of Standards, not subject to copyright.

[1] Experiments with stored beams have been done earlier; for example, an experiment using cesium is described in Ref. [4].

calibrate the intensity of the hydrogen beam. We then used the beam system of the maser oscillator to evaluate the performance of our hydrogen atom detector.[2]

The beam intensity at oscillation threshold of the hydrogen maser [7] is given by

$$I_{th} = c\,\gamma_o^2 \qquad (3)$$

with $c \equiv hV/8\pi^2\mu_o^2 Q\eta$, where V is the volume, Q the loaded quality factor, and η the filling factor [7] of the cavity; μ_o is the magnetic dipole moment of the transition, h is Planck's constant, and γ_o the relaxation constant. One has to distinguish carefully between the relaxation of the population difference described by γ_1, and the relaxation of the oscillating magnetic moment described by γ_2. It can be shown that [8]

$$\gamma_o^2 = \gamma_1\gamma_2 \qquad (4)$$

where γ_1 and γ_2 are each the sum of all corresponding relaxation processes. We now assume that all relaxation processes other than hydrogen-hydrogen spin exchange can be described by $\gamma_{1t} = \gamma_{2t}$ and that for spin-exchange $\gamma_{1SE} = 2\gamma_{2SE}$ [8]. This allows us to rewrite eq (4):

$$\gamma_o^2 = \gamma_2^2\left(1 + \frac{\gamma_{2SE}}{\gamma_2}\right). \qquad (5)$$

If γ_o is measured, the threshold beam intensity can be calculated from eq (3) since the constant c is known.[3] The relaxation constants can be measured by observing the decay of the radiation intensity in the maser cavity after applying a suitable, stimulating microwave pulse. The maser cavity was equipped with two coupling loops; the pulse was applied to one, the radiative decay observed at the other using a three-stage superheterodyne receiver. The pulse was generated by pulsing a frequency synthesizer whose frequency (about 20 MHz) was subtracted from quartz crystal controlled 1440 MHz to match the atomic hydrogen resonance frequency. Two important items must be considered: (1) When pulsed, the maser must be far below oscillation threshold. (2) Only γ_2 is directly observable; in order to obtain γ_o [see eq (5)] one must also determine γ_{2SE}. The following measurement procedure was therefore established: (a) the maser was made to oscillate; (b) the maser was tuned to maximum oscillation amplitude; (c) the maser oscillator was brought as accurately as possible to oscillation threshold by introducing a suitable inhomogeneity in the axial DC magnetic field in order to fulfill the conditions on which eq (3) is based; (d) the maser was brought far below oscillation threshold by detuning the microwave cavity, γ_2 was measured by observing the pulse decay (Fig. 1a); (e) the hydrogen beam intensity was reduced to a level where no spin-exchange occurred, the pulse decay was again measured (Fig. 1b), and γ_{2SE} was obtained as the difference between this measurement and the one according to (d) above; (f) I_{th} was calculated using eqs (3) and (5).

We used this procedure to measure the beam intensity as a function of the atomic hydrogen source parameters. The source was a pyrex glass bottle with a collimator opening consisting of a bundle of channels with about 40 μm diameter each and a length of 0.6 mm. The total diameter of the bundle was 1.3 mm. The dissociating discharge was driven by a 200-MHz RF generator. Figure 2a shows that the beam intensity[4] depends linearly on the source pressure at constant RF power, and reaches more than 10^{12} atoms per second. It should be noted that typical beam intensities for hydrogen maser oscillator operation are about 10^{11} atoms per second. Figure 2b depicts the dependence of the beam intensity on the RF power of the discharge at constant source pressure. This curve essentially shows the degree of dissociation into atomic hydrogen and indicates a leveling off of the dissociation with higher RF power.

The atomic hydrogen detector was a commercial residual gas analyzer, i.e., an electron bombardment ionizer followed by a quadrupole mass spectrometer and an electron multiplier. The ionizer emits a sheet of electrons, about 2 mm high (along the beam axis), across the hydrogen beam. For highest ionization efficiency, the electron voltage is chosen to yield the maximum ionization cross-section for hydrogen (approx. 70 V). We measured the electron multiplier gain and obtained from the comparison between the detected current and the calibrated hydrogen beam intensity (corrected for geometrical factors, and the presence of atoms in the F = 1, m = 1 level) an efficiency of 1.5×10^{-5} at an electron emission current of 1 mA. The efficiency increased nearly linearly with the electron current to reach 5×10^{-5} at maximum emission current (3 mA).[5]

1.2 Operation of the beam

The hydrogen storage beam tube system which we used is shown in Fig. 3. A hydrogen maser oscillator was modified by adding a second output opening to the storage bulb, followed by a dipole magnet as the second state selector and the atomic hydrogen detector which was positioned at the proper deflection angle. A beam stop was placed in the center of the bulb to prevent the direct passage of the hydrogen beam. Differential pumping decoupled the detector vacuum chamber from the main vacuum chamber by about a factor of 10^{-4}. In operation, the vacuum at the detector was measured to be approximately 10^{-10} torr ($\approx 10^{-8}$ N/m^2).

[2] Care has to be taken that identical geometries are used in the maser oscillator mode and in the particle detection mode. In our experiments we always used a 4-mm diameter circular aperture at the entrance of the storage bulb or the detector entrance, respectively, and always positioned at a distance of 45 cm from the exit of the state selector magnet.

[3] In our maser we had V = 0.0137 m^3, Q = 28 000, η = 3.5.

[4] The beam intensity is always measured after the aperture mentioned in footnote 2. Also, it must be noted that we are only observing the difference in the intensities of the F = 1, m = 0 and F = 0, m = 0 states.

[5] The massresolution of the mass spectrometer was chosen to be as low as possible in order to increase the overall efficiency.

We first tested our system with a direct hydrogen beam (beam stop removed). A microwave signal was swept across the hydrogen resonance and the detector current measured. The resulting resonance curve with a linewidth of about 10 kHz is depicted in Fig. 4. A post-detection bandwidth of about 1 Hz was used. The ionizer efficiency was set at about 2.5×10^{-5}.

For the case of storage of hydrogen in the bulb we estimated an efficiency of 10^{-3} in the reformation of an exiting beam, i.e., we expected a beam intensity of about 10^{9} atoms per second at the detector with an initial beam intensity at the input of the storage bulb of 10^{12} atoms per second. Thus, with a detector efficiency of about 10^{-5} the detected particle count was expected to be marginal with only about 10^{4} atoms per second. Nevertheless, we operated such a complete system (Fig. 3) and detected a microwave response in the beam intensity with a signal-to-noise ratio of about one to one at 100 s averaging time. The limiting noise was apparently shot noise due to an atomic hydrogen background. This background is produced by dissociation of residual, hydrogen-containing gases in the system as well as molecular hydrogen which diffuses from the source to the detector region or, more important, is produced by the hot metal components of the detector (mostly stainless steel) itself. We tried a more efficient ionizer with a space charge limited electron emission current of 50 mA. The efficiency was measured to be 5×10^{-4}, but its application as a detector brought no advantage because of its correspondingly larger background signal. A reduction in the electron accelerating voltage of the ionizer will reduce the background. However, the ionization cross-section of hydrogen diminishes correspondingly, and the signal to noise remains nearly unchanged.[6]

We judged from these results that a major effort on the design of the exiting beam system (beam optics and detector) was called for. In view of our limited resources we decided to temporarily discontinue this work and to proceed with the alternate detection method: microwave detection.

2. Microwave Detection

2.1 Apparatus

The block diagram of our apparatus is depicted in Fig. 5. The 5-MHz signal from a quartz crystal oscillator is multiplied by a factor of 288 and mixed with a signal from a synthesizer (about 19.594 MHz) to generate a signal at approximately the hydrogen transition frequency. This signal, which can be swept across the hydrogen resonance by sweeping the synthesizer frequency, is transmitted through the microwave cavity and mixed again with the signals from the multiplier and synthesizer. Amplification before the last mixing yields a good output at the last mixer (phase-sensitive detector) thus avoiding possible limitations due to low frequency noise (flicker noise) in the output of the phase-sensitive detector and in the circuits following it. Not shown in Fig. 5 are the isolators, necessary to decouple the circuits connected to the output of the microwave cavity from those at its input, and the phase-shifters.

The output of the phase-sensitive detector is proportional to the imaginary part of the total complex cavity response. If the cavity contains state-selected hydrogen atoms and is tuned to their transition frequency, the hydrogen resonance is observable at the output of the phase-sensitive detector as a phase-change due to the corresponding dispersion. In order to obtain the frequency pulling factor of eq (2), i.e., in order to subtract the cavity response, we modulate the hydrogen beam intensity at a relatively low rate, e.g., 1 Hz. The output of the phase-sensitive detector which contains the phase information about the hydrogen resonance (now modulated also at 1 Hz) is fed into a synchronous detector ("lock-in amplifier"). Its amplified and filtered output serves as the correcting voltage for the crystal oscillator. The locking criterion is thus a nulling of the phase-change under modulation of the intensity of the hydrogen beam entering the cavity. The hydrogen beam apparatus resembles closely a conventional hydrogen maser oscillator except for the lower cavity-Q which places it significantly below threshold (see Section 2.2).

At this point it should be noted that in storage devices such as ours, the strength of the signal due to the hydrogen atoms as well as the associated linewidth will increase as the interrogating power increases; there is no optimum power [6], [9] as in beam tubes (see Appendix). In the Appendix we show that a typical power P_t can be defined for which the transition probability is 1/4 and the linewidth is

$$W_t = \frac{\sqrt{2}}{\pi} \gamma_e \qquad (6)$$

where γ_e is the escape relaxation constant for the stored hydrogen atoms. All other relaxation processes are here assumed to be insignificant. This assumption is a good approximation if relatively short escape relaxation times are used (see below).

2.2 Experiments

We used in our first experiments a storage bulb of 10 cm diameter with a relatively short excape relaxation time (calculated) of 0.1 s. The corresponding linewidth at the typical power P_t follows from eq (6) as $W_t = 4.5$ Hz. We operated at beam intensities which are comparable to those used in hydrogen maser oscillators. From previous experience we know that the cavity-Q for an oscillation threshold beam intensity I_{th} at storage times of about 1 s is approximately 30 000. Since the oscillation threshold condition depends on the square of the storage time [eq (3)], the (fictitious) threshold cavity-Q for our device operating at beam intensities of about 30 I_{th} is approximately $Q_{c,th} \approx 90\,000$. We reduced our cavity-Q to $Q_c \approx 2500$ by over-critically coupling to the output load of the cavity. Thus, our system was operating at the fraction $\alpha = Q_c/Q_{c,th} \approx 0.028$ of oscillation threshold.

[6] We obtained a maximum in the signal to noise at about 23 V accelerating voltage. This maximum is about 2.5 times larger than the signal to noise at 70 V accelerating voltage. However, the ionizer efficiency at 23 V accelerating voltage is only about one-half of the value at 70 V.

From eq (2) we calculate the pulling factor to be $F \approx 4 \times 10^{-6}$. This is one order of magnitude less than in the case of a typical hydrogen maser oscillator. Since environmental temperature fluctuations are the dominant cause for cavity frequency fluctuations, the above pulling factor puts us close to a fractional frequency change of 1×10^{-12} per degree kelvin for our device due to its fused quartz cavity.[7]

The hydrogen dispersion signal, as measured at the output of the phase-sensitive detector, is depicted in Fig. 6. The horizontal scale is indicated on the figure; the recording was made with a post-detection time constant of 10^{-3} s; the hydrogen beam was not modulated. A high-resolution recording of the output signal of the synchronous detector is shown in Fig. 7. The horizontal scale is shown on the figure; a post-detection time constant of 10 s was used. The hydrogen beam was modulated by turning the hydrogen discharge in the source on and off at a 1-Hz frequency. The linewidth of about 5 Hz agrees with the predicted value.

We operated the system as a frequency standard, i.e., we locked the crystal oscillator to the resonance, as shown in Fig. 5. The frequency stability was measured against (commercial) cesium clocks used in the NBS time scale and against crystal oscillators. A typical result is depicted in Fig. 8 where the square root of the two-sample Allan variance [10] is plotted versus the sampling time. The circles are values obtained against a cesium clock; the triangles represent a measurement against a crystal oscillator. The best stabilities, with values of 4×10^{-13}, were measured at sampling times of $\tau = 30$ s and of $\tau = 3$ hours. Basically, Fig. 8 depicts the performances of a particular crystal oscillator and a particular cesium beam frequency standard. The instability due to the atomic hydrogen storage beam frequency standard does not show up, i.e., its performance apparently is equal to--or possibly better than--the crystal oscillator and the cesium beam frequency standard in their respective ranges.

Conclusions

We have described hydrogen storage beam devices based on hydrogen atom detection as well as on microwave detection. Theoretically, hydrogen atom detection leads to a device of superior performance; however, inefficient detection and high background so far have prevented us from completing such a frequency standard. Nevertheless, the concept appears promising: Straightforward improvements in the efficiency of the beam optics and the detector to an overall efficiency of at least 10^{-5}, as well as a reduction in the hydrogen background, appear feasible. Also, other detection principles could be utilized, e.g., detection based on the comparatively high recombination energy of hydrogen. We plan to resume work along these lines.

Dispersion-locking of a crystal oscillator to the atomic hydrogen hyperfine resonance resulted in a frequency standard with a promising frequency stability performance. The reduced cavity pulling factor may lead to improved long-term frequency stability and/or to a simplified design of the apparatus as compared to the hydrogen maser oscillator. The cavity pulling factor could be reduced to the point where the second-order Doppler effect (1.4×10^{-13} per degree) would determine the requirements for thermal stabilization. The wall-shift may become more conveniently evaluable; for this, cavity pulling could be reduced further to allow changes of the shape of the storage bulb without the need for retuning the cavity [11], [12] or perhaps with a simple resetting of the cavity by external sensing of the detuning.

The spin exchange frequency shift enters explicitly as a frequency bias which must be evaluated and which can be evaluated with the device described in this paper. However, this bias is expected not to exceed a few parts in 10^{13} for typical operating conditions [13], and its direct, precise measurement appears to be desirable in view of some doubts about the total validity of the compensation of spin exchange shift by cavity pulling in the cavity tuning procedure of the maser oscillator [14].

Acknowledgements

The authors would like to thank Roxanne M. Pierce and James A. Morgan for their dedicated help in construction and measurements. We appreciate the assistance of David W. Allan in the frequency stability comparisons and stimulating discussions with Günter Kramer and Donald Halford which helped shape this paper.

Appendix

The probability density f(t) for an atom to stay for some time t in the storage bulb is given by

$$f(t) = \gamma_e e^{-\gamma_e t} \tag{7}$$

where γ_e is the escape relaxation constant.[8]

This exponential distribution function leads easily to the transition probability T for an ensemble of stored atoms [7].

$$T = \frac{\frac{1}{2} x^2}{(\omega - \omega_o)^2 + \gamma_e^2 + x^2} \tag{8}$$

where

$$x = -\frac{\mu H}{\hbar} . \tag{9}$$

[7] In our experiments the cavity was not thermally controlled.

[8] Strictly, eq (7) cannot be completely true because we have a cutoff at very short times due to the physical necessity for the atoms to traverse the storage bulb at least once before escaping.

In eq (9), μ is the magnetic dipole moment of the transition and H is the average microwave signal amplitude in the interrogation region. The power delivered by the atoms to the cavity is then $nT\hbar\omega_o$ where n is the flux of atoms in the upper state minus the flux of atoms in the lower state. We see that at resonance T has no maximum but approaches asymptotically T = 1/2 for arbitrarily large excitation ($x \to \infty$).

The line will broaden with increasing excitation. From eq (8) we get for the linewidth

$$W = \frac{1}{\pi}(\gamma_e^2 + x^2)^{\frac{1}{2}} . \qquad (10)$$

We define a typical microwave power P_t with a corresponding perturbation parameter x_t and a linewidth W_t by setting

$$x_t^2 = \gamma_e^2 . \qquad (11)$$

This leads to $T_t = 1/4$ at resonance, and $W_t = \frac{\sqrt{2}}{\pi}\gamma_e$.

References

[1] J. Viennet, C. Audoin, and M. Desaintfuscien, Proc. 25th Annual Symposium on Frequency Control, Fort Monmouth, N.J., 337 (1971). Available from Electronics Industries Association, Washington, D.C.

[2] H. Hellwig, Metrologia 6, 56 (1970).

[3] For a listing of most experiments up to 1970 which involve the wallshift, see: H. Hellwig, R.F.C. Vessot, M. Levine, P. W. Zitzewitz, D. W. Allan, and D. J. Glaze, IEEE Trans. Instr. and Meas. IM-19, 200 (1970).

[4] H. M. Goldenberg, D. Kleppner, and N. F. Ramsey, Phys. Rev. 123, 530 (1961).

[5] H. Hellwig, Metrologia 6, 119 (1970).

[6] J. H. Holloway and R. F. Lacey, Proc. Congrès International de Chronométrie, Lausanne, Vol. 1, 317 (1964).

[7] D. Kleppner, H. M. Goldenberg, and N. F. Ramsey, Phys. Rev. 126, 603 (1962).

[8] H. Hellwig, Phys. Rev. 166, 4 (1968).

[9] N. F. Ramsey, Molecular Beams. Oxford: Clarendon 1956, p. 118ff.

[10] D. W. Allan, Proc. IEEE 54, 221 (1966); also J. A. Barnes et al., IEEE Trans. Instr. and Meas. IM-20, 105 (1971).

[11] P. E. Debély, Proc. 24th Annual Symposium on Frequency Control, Fort Monmouth, N.J., 259 (1970). Available from Electronics Industries Association, Washington, D.C.

[12] D. Brenner, J. Appl. Phys. 41, 2942 (1970).

[13] H. Hellwig, NBS Technical Note No. 387 (1970).

[14] S. B. Crampton, J.A. Duvivier, G.S. Read, and E.R. Williams, Phys. Rev. A5, 1752 (1972).

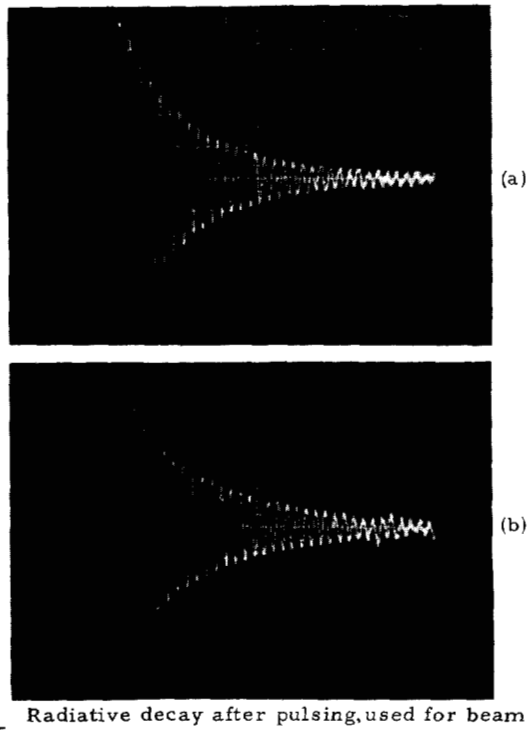

Fig. 1 Radiative decay after pulsing, used for beam intensity calibration. (a) decay under oscillation threshold conditions, (b) decay at reduced beam intensity for determination of the spin-exchange relaxation. Horizontal scale: 0.1 s per division.

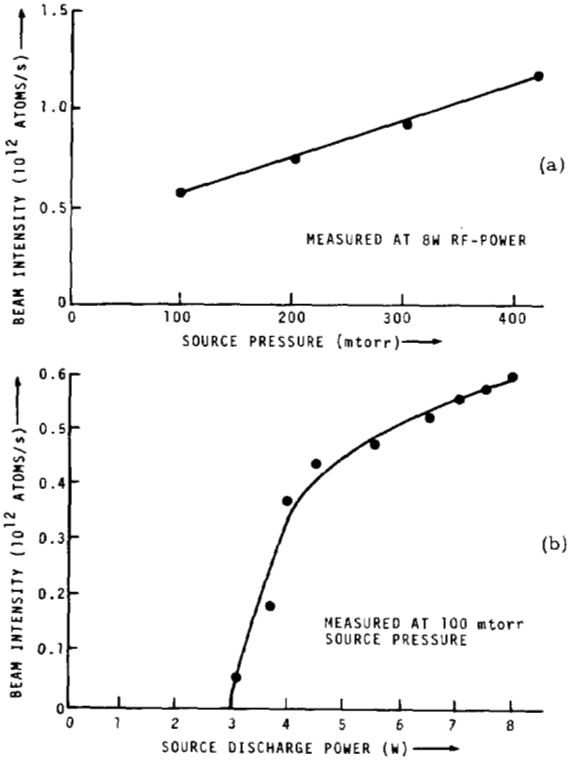

Fig. 2 (a) Beam intensity as a function of the hydrogen pressure in the source; RF power held constant, (b) beam intensity as a function of the RF discharge power in the source; source pressure held constant. The numerical values for the pressure are uncorrected readings of a thermocouple gauge.

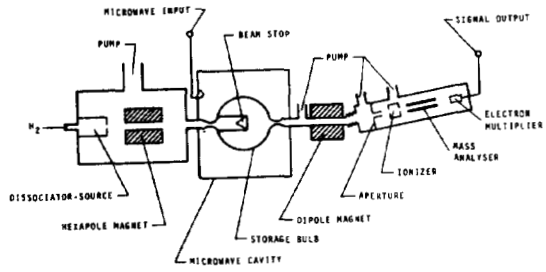

Fig. 3 Schematic of the hydrogen storage system with detection of atomic hydrogen.

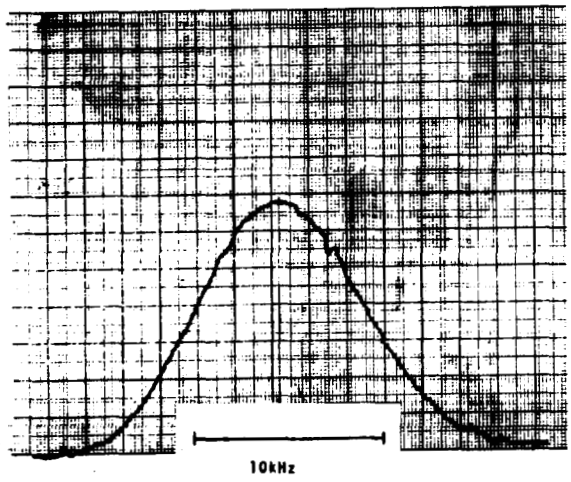

Fig. 4 Hydrogen hyperfine resonance in a free hydrogen beam; obtained by hydrogen atom detection. Post-detection bandwidth: 1 Hz.

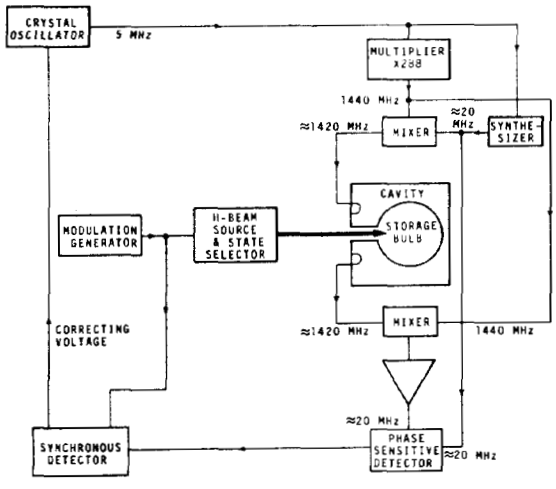

Fig. 5 Block diagram of the atomic hydrogen storage beam frequency standard. Phase-shifters and isolation devices not shown.

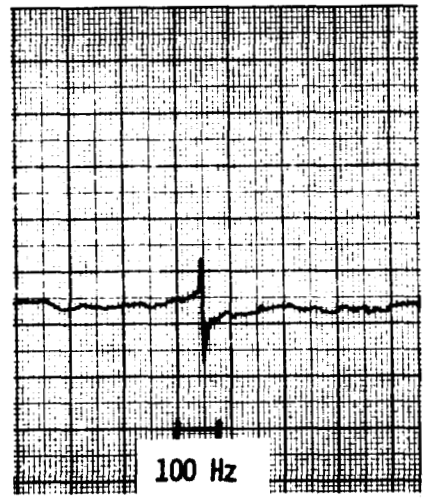

Fig. 6 Hydrogen dispersion signal as measured at the output of the phase-detector (open-loop operation). No beam modulation. Recording time constant: 10^{-3} s. Sweep speed: 5.6 Hz/s.

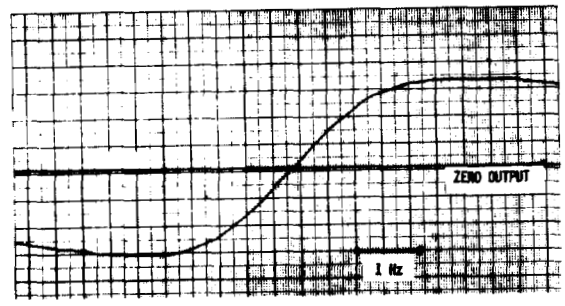

Fig. 7 Hydrogen dispersion signal as measured at the output of the synchronous detector (open-loop operation). Beam modulated at 1 Hz. Recording time constant: 10 s. Sweep speed: 0.022 Hz/s.

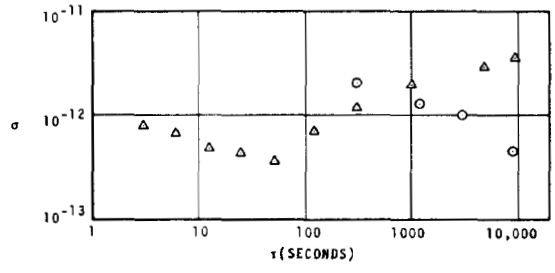

Fig. 8 Frequency stability of the device of Fig. 5 measured against a crystal oscillator (triangles) and a cesium beam frequency standard (circles). The square root of the Allan variance $\sigma_y^2(N, T, \tau, B)$ is plotted where: number of samples $N = 2$, deadtime $T - \tau = 0$, and bandwidth $B = 30$ Hz. The sampling time τ is the variable, and y denotes fractional frequency fluctuations.